J Comput Electron (2007) 6:179–182
DOI 10.1007/s10825-006-0077-7

A multi-purpose Schrödinger-Poisson Solver for TCAD applications

Markus Karner · Andreas Gehring · Stefan Holzer · Mahdi Pourfath · Martin Wagner · Wolfgang Goes · Martin Vasicek · Oskar Baumgartner · Christian Kernstock · Klaus Schnass · Gerhard Zeiler · Tibor Grasser · Hans Kosina · Siegfried Selberherr

Published online: 26 January 2007

Abstract We present the Vienna Schrödinger-Poisson Solver (VSP), a multi-purpose quantum mechanical solver for investigations on nano-scaled device structures. VSP includes a quantum mechanical solver for closed as well as open boundary problems on fairly arbitrary one-dimensional cross sections within the effective mass framework. For investigations on novel gate dielectrics VSP holds models for bulk and interface trap charges, and direct and trap assisted tunneling. Hetero-structured semiconductor devices, like resonant tunneling diodes (RTD), can be treated within the closed boundary model for quick estimation of resonant energy levels. The open boundary model allows evaluation of current voltage characteristics.

M. Karner (✉)
Institute for Microelectronics, TU Wien, Gußhausstraße 27–29, A-1040 Vienna, Austria
e-mail: markus.karner@iue.tuwien.ac.at

A. Gehring
AMD Saxony, Wilschdorfer Landstrasse 101, D-01109 Dresden, Germany
e-mail: andreas.gehring@amd.com

S. Holzer · M. Pourfath · M. Wagner · W. Goes · M. Vasicek · O. Baumgartner · C. Kernstock · K. Schnass · G. Zeiler · T. Grasser · H. Kosina · S. Selberherr
Institute for Microelectronics, TU Wien, Gußhausstraße 27–29, A-1040 Vienna, Austria
e-mail: grasser@iue.tuwien.ac.at

H. Kosina
e-mail: kosina@iue.tuwien.ac.at

S. Selberherr
e-mail: selberherr@iue.tuwien.ac.at

Keywords Simulation · Schrödinger-Poisson solver · Quantum transport · Nanoelectronic devices

1 Introduction

Numerous technological innovations, including material and process changes such as high-k gate dielectrics and metal gate electrodes, are investigated to meet the upcoming scaling requirements. Furthermore, novel structures such as ultra-thin body and multiple-gate MOSFETs are expected to be introduced to suppress short-channel effects [1]. To overcome the technological problems, further theoretical and experimental research has to be performed which requires an extensive use of computer simulation. We developed the Vienna Schrödinger Poisson solver (VSP), a multi-purpose quantum mechanical solver with the aim to aid theoretical as well as experimental research on nano-scale electronic devices.

2 The models

This section briefly describes the models implemented in the Schrödinger Poisson (S/P) solver. The chosen software architecture allows to add new models easily. VSP is a quantum mechanical solver for closed as well as open boundary problems. The thereby calculated carrier concentration is used in the Poisson equation in a self consistent manner.

2.1 The Poisson model

The Poisson equation describes the relation between the electrostatic potential φ and the space charge ρ.

$$\nabla \cdot (\varepsilon \nabla \varphi) + \rho(\varphi) = 0$$

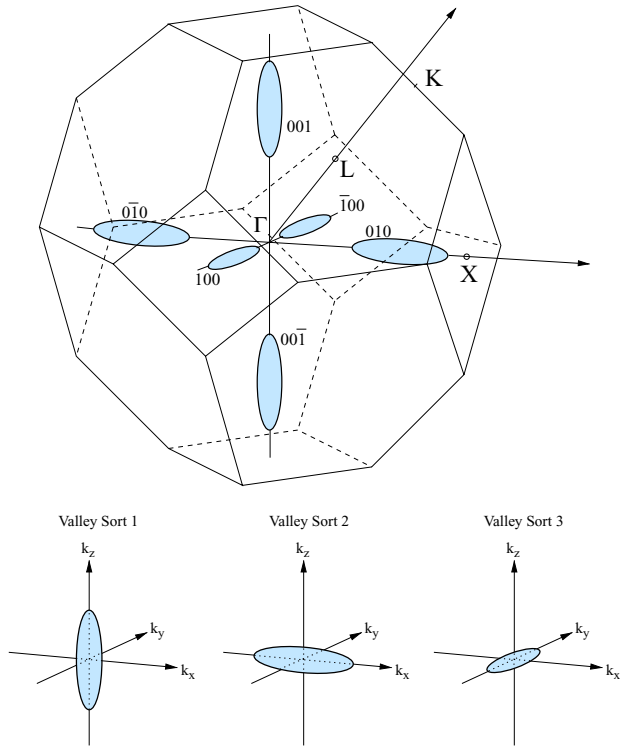

Fig. 1 Equi-energy surfaces of the first conduction band of unstrained Silicon. VSP treats the conduction band as three valleys having the same minimum energy but different orientations of the effective mass tensor as shown in the lower part of the figure

Hence, for S/P calculations a system of coupled partial differential equations (PDE) has to be solved self-consistently. We use an iterative predictor corrector scheme [2] in order to achieve a fast and stable convergence behavior. For each iteration step i, a linearized Poisson equation has to be solved:

$$\nabla \cdot (\varepsilon \nabla \varphi^i) + \varphi^i \frac{\partial \rho}{\partial \varphi}\bigg|_{\varphi^{i-1}} = -\rho(\varphi^{i-1}).$$

2.2 Effective mass approach

The band structure for electrons and holes is given by an arbitrary number of valley sorts, defined by an anisotropic effective mass and a band edge energy [3] (see Fig. 1). In this way a wide range of materials can be treated. Also, the effects of substrate orientation as well as strain on the band structure are taken into account.

Assuming a three-dimensional electron gas, effective mass approximation, and Fermi statistics, the carrier concentration is determined by the distance of Fermi energy and conduction band:

$$n_{3D}(x) = N_{C,3D}\, \mathcal{F}_{C,1/2}\left(\frac{\mathcal{E}_F - \mathcal{E}_c}{k_B T}\right).$$

Here $\mathcal{F}_{C,1/2}$ denotes the complete Fermi Function of the order 1/2 and $N_{C,3D}$ the effective density of states (DOS).

2.3 Closed system S/P

The energy levels $\mathcal{E}_n$ as well the wave functions Ψ_n of bound states within a quantum well follows from the effective mass Schrödinger equation:

$$\left(-\frac{\hbar^2}{2m}\frac{\partial^2}{\partial x^2} + V(x)\right)\Psi(x) = \mathcal{E}\,\Psi(x)\,.$$

For a well with a finite height $\mathcal{E}_{lim}$ (e.g. MOS inversion layer), the occupation of the subband states is considered up to this energy $\mathcal{E}_{lim}$. The electron density is given by the effective DOS of a two-dimensional electron gas $N_{C,2D}$ and the incomplete Fermi Function:

$$n_{2D}(x) = N_{C,2D} \sum_n |\Psi_n(x)|^2 \times \left(\mathcal{F}_{I,0}\left(\frac{\mathcal{E}_F - \mathcal{E}_n}{k_B T}, 0\right) - \mathcal{F}_{I,0}\left(\frac{\mathcal{E}_c - \mathcal{E}_F}{k_B T}, \frac{\mathcal{E}_n - \mathcal{E}_{lim}}{k_B T}\right)\right).$$

Starting at $\mathcal{E}_{lim}$, a continuum of states is assumed, which gives rise to an electron density

$$n_{3D}(x) = N_{C,3D}\, \mathcal{F}_{I,1/2}\left(-\frac{\mathcal{E}_c - \mathcal{E}_F}{k_B T}, -\frac{\mathcal{E}_{lim} - \mathcal{E}_c}{k_B T}\right).$$

The total electron density n writes as the sum of the two contributions: $n = n_{2D} + n_{3D}$.

2.4 Bulk and interface trap charges

VSP includes models for interface traps and bulk traps in arbitrarily stacked gate dielectrics. The occupation of the interface states g_{int} is calculated using Fermi statistics and gives rise to a surface charge given by

$$\rho_{int} = q \int_{\mathcal{E}_{min}}^{\mathcal{E}_{max}} g_{int}(\mathcal{E})\, f(\mathcal{E})\, d\mathcal{E}\,.$$

2.5 Direct tunneling current

Following [4], the direct tunneling current components from both, continuum J_{3D} and quasi bound states (QBS) J_{2D}, can

be estimated by

$$J_{\mathrm{d,2D}} = \mathrm{q} \sum_j \frac{n_i}{\tau_i},$$

$$J_{\mathrm{d,3D}} = \mathrm{q} \int_{\mathcal{E}_{\mathrm{lim}}}^{\mathcal{E}_{\mathrm{max}}} TC(\mathcal{E}_x, m_{\mathrm{diel}}) N(\mathcal{E}_x, m_{\mathrm{D}})\, \mathrm{d}\mathcal{E}_x .$$

2.6 Trap assisted tunneling current

Trap assisted tunneling (TAT), which is a major issue regarding reliability in novel gate stacks [6], is taken into account in terms of an inelastic single step tunneling process [7]. The current density reads:

$$J_{\mathrm{tat}} = \mathrm{q} \int_{d_1}^{d_2} \frac{N_{\mathrm{tat}}(x)}{\tau_{\mathrm{c}}(x) + \tau_{\mathrm{e}}(x)}\, \mathrm{d}x.$$

2.7 Open system S/P

For systems dominated by quantum ballistic transport, like resonant tunneling diodes (RTD), an open boundary solver using the non equilibrium Green's function formalism [8] is available.

$$G^R_{\mathbf{r},\mathbf{r}'}(\mathcal{E}) = [\mathcal{E} I - H_{\mathbf{r},\mathbf{r}'} - \Sigma^R_{\mathbf{r},\mathbf{r}'}(\mathcal{E})]^{-1}$$

$$G^{<,>}_{\mathbf{r},\mathbf{r}'}(\mathcal{E}) = G^R_{\mathbf{r},\mathbf{r}'}(\mathcal{E}) \Sigma^{<,>}_{\mathbf{r},\mathbf{r}'}(\mathcal{E}) G^A_{\mathbf{r},\mathbf{r}'}(\mathcal{E})$$

$$j_{\mathbf{r},\mathbf{r}'} = \frac{2q}{\hbar} \int 2Re\{G^<_{\mathbf{r},\mathbf{r}'}(\mathcal{E}) H_{\mathbf{r},\mathbf{r}'}\} \frac{d\mathcal{E}}{2\pi}$$

$$n_{\mathbf{r},\mathbf{r}} = -2i \int G^<_{\mathbf{r},\mathbf{r}}(\mathcal{E}) \frac{d\mathcal{E}}{2\pi}$$

For types of Green's functions are defined. $G^{R,A}$ deal with the dynamics of carriers and $G^{<,>}$ with the statistics of carriers. We use an adaptive method to generate a nonuniform mesh in the energy-space. Very narrow resonances are resolved, while the total number of grid points is kept low, thus delivering stable results at reasonable simulation times [9].

3 Software techniques

The software is written in C++ using state-of-the-art software design techniques. Critical numerical calculations are performed with stable and powerful numerical libraries Blas, Lapack, and Arpack. VSP holds a graphical user interface written in Java (see Fig. 3), as well as an XML based interface. Furthermore, VSP has an open software application interface (API) for the use inside third party simulation environments. These features are mandatory for tasks like parameter identification and model calibration, e.g. for CV curves and gate stack optimizations [10]. Binaries are available for Linux, Windows, IBM AIX, and MacOS on request.

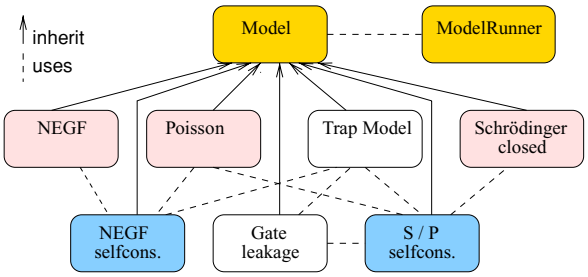

Fig. 2 VSP is structured into several models having a common interface. Hence, new models can be added easily without any change in the existing software architecture

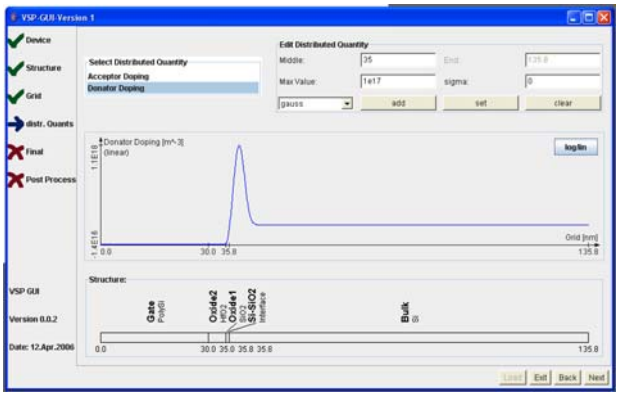

Fig. 3 The user is guided through the simulation process by the GUI. The steps are device definition, grid specification, quantity definition, select and run the proper model, and finally the evaluation of the simulation results. A screen shot of the distributed quantity editor is shown

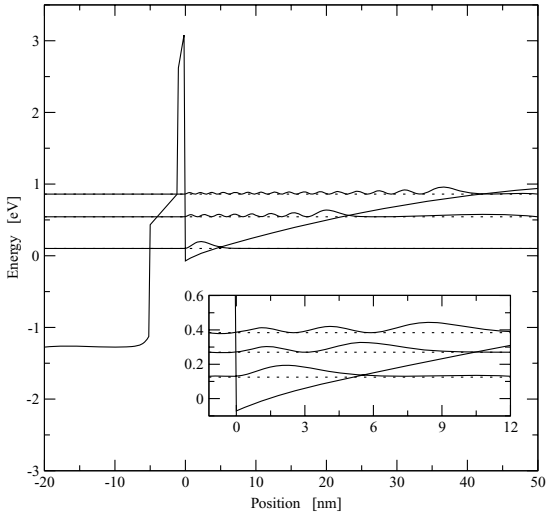

Fig. 4 The wavefunctions and the energy levels of some QBS in the inversion layer of an nMOS device with a stacked gate dielectric

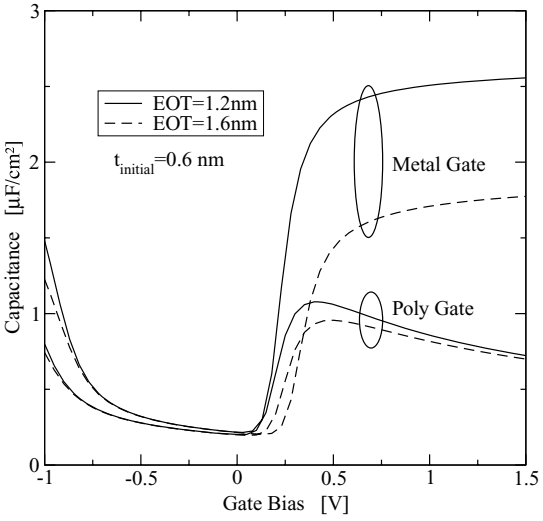

Fig. 5 The CV characteristic of SiO_2 HfO_2 stacked gate dielectric for different EOTs. An initial SiO_2 layer of 0.6 nm has been assumed. The use of metal gates is reasonable for down scaling the EOT to the sub 1.0 nm

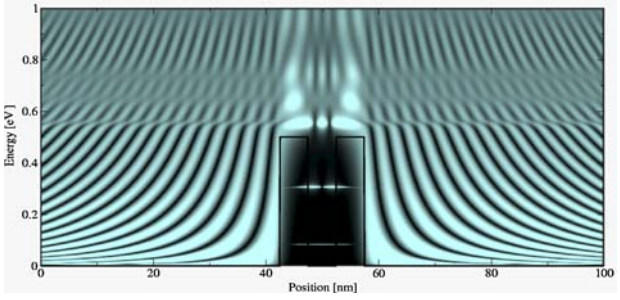

Fig. 6 Local density of states of a resonant tunneling diode (RTD) at zero bias. Quantized states are clearly shown in the well

4 Applications

For investigations of MOS inversion layers, a closed boundary solver is applied. The calculation of leakage currents is performed in a post processing step, since they have a negligible influence on the electrostatic device behavior. Conventional bulk MOS, partially depleted SOI as well as novel device designs like DG-MOS structures can be investigated. The band edge energy of a MOS structure with a stacked gate

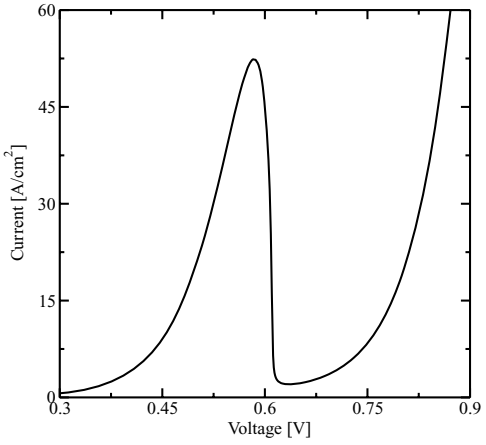

Fig. 7 IV characteristics of an RTD with open boundary conditions. The negative differential resistance can be clearly seen

dielectric under inversion conditions has been evaluated and displayed in Fig. 4. The corresponding CV characteristic is shown in Fig. 5. A resonant tunneling diode has been investigated using the open boundary S/P solver model. For the double barrier structure, a barrier height of 0.5 eV, a barrier width of 2 nm, and a quantum well width of 2 nm has been assumed. The local density of states and the IV characteristics are shown in Figs. 6 and 7, respectively.

Acknowledgment This work has been partly supported by the European Commission, project SINANO, IST 506844 and from the Austrian Science Fund, special research project IR-ON (F2509-N08).

References

1. Semiconductor Industry Association, International Technology Roadmap for Semiconductors - 2005 Update (2005)
2. Trellakis, A., et al.: J. Appl. Phys. **81**(12), 7880–7884 (1997)
3. Stern, F.: Physical Review B **5**, 4891 (1972)
4. Gehring, A., et al.: IEEE Transactions on Device and Materials Reliability. **4** (3), 306–319 (2004)
5. Karner, M., et al.: Proc. MSED 2005. 97–98 (2005)
6. Houssa, M., et al.: J. Appl. Phys. **87**(12), 8615–8620 (2000)
7. Jiménez-Molinos, F., et al.: J. Appl. Phys. **90** (7), 3396–3404 (2001)
8. Datta, S.: Superlattices and Microstructures **28**, 253–278 (2000)
9. Pourfath, M., et al.: Proc. MSED 2005. 95–96 (2005)
10. Holzer, S., et al.: SNDT 2004, 113–116 (2004)